22. White, E. *et al*. Adenovirus E1B 19-kilodalton protein overcomes the cytotoxicity of E1A proteins. *J. Virol.* **65,** 2968–2978 (1991).
23. Kahana, J. & Silver, P. in *Current Protocols in Molecular Biology* (eds Ausubel, F. M. *et al.*) 9.7.22–9.7.28 (Greene and Wiley Interscience, New York, 1996).
24. Zhu, L. *et al*. Inhibition of cell proliferation by p107, a relative of the retinoblastoma protein. *Genes Dev.* **7,** 1111–1125 (1993).
25. Ausubel, F. M. *et al. Current Protocols in Molecular Biology* (Greene and Wiley Interscience, New York, 1996).
26. Krek, W., Livingston, D. M. & Shirodkar, S. Binding to DNA and the retinoblastoma gene product promoted by complex formation of different E2F family members. *Science* **262,** 1557–1560 (1993).
27. Chittenden, T., Livingston, D. M. & DeCaprio, J. A. Cell cycle analysis of E2F in primary human T cells reveals novel E2F complexes and biochemically distinct forms of free E2F. *Mol. Cell. Biol.* **13,** 3975–3983 (1993).
28. Friedlander, P *et al*. A mutant p53 that discriminates between p53-responsive genes cannot induce apoptosis. *Mol. Cell. Biol.* **16,** 4961–4971 (1996).
29. Qin, X.-Q. *et al*. The transcription factor E2F-1 is a downstream target of RB action. *Mol. Cell. Biol.* **15,** 742–755 (1995).
30. Somasundaram, K. & El-Deiry, W. S. Inhibition of p53-mediated transactivation and cell cycle arrest by E1A through its p300/CBP-interacting region. *Oncogene* **14,** 1047–1057 (1997).

Acknowledgements. We thank everyone who provided reagents used in this study; J. Kahana, P. Silver, C. Jost and W. G. Kaelin Jr for providing unpublished reagents; P. Adams, R. Eckner, M. Ewen, O. Iliopoulos, R. Scully, T.-P. Yao and members of the Division of Neoplastic Disease Mechanisms for discussions; M. Modabber for graphics; and M. Simone for flow cytometry. This work was supported by grants from the American Cancer Society (N.L.L.), the Howard Hughes Medical Institute (S.R.G.), The Cancer Research Fund of the Damon Runyon–Walter Winchell Foundation (D.G.), the Dana-Farber/Sandoz Drug Discovery Program, and the National Cancer Institute (J. DeC. and D.M.L.).

Correspondence and requests for materials should be addressed to D.M.L. (e-mail: david_livingston @dfci.harvard.edu).

Structure of isopenicillin *N* synthase complexed with substrate and the mechanism of penicillin formation

Peter L. Roach*, Ian J. Clifton*, Charles M. H. Hensgens*, Norio Shibata*, Christopher J. Schofield*, Janos Hajdu† & Jack E. Baldwin*

** The Dyson Perrins Laboratory and the Oxford Centre of Molecular Sciences, University of Oxford, South Parks Road, Oxford OX1 3QY, UK*
† Department of Biochemistry, Biomedical Centre, Uppsala University, Box 576, S-751 23 Uppsala, Sweden

The biosynthesis of penicillin and cephalosporin antibiotics in microorganisms requires the formation of the bicyclic nucleus of penicillin[1]. Isopenicillin *N* synthase (IPNS), a non-haem iron-dependent oxidase, catalyses the reaction of a tripeptide, δ-(L-α-aminoadipoyl)-L-cysteinyl-D-valine (ACV), and dioxygen to form isopenicillin *N* and two water molecules[2]. Mechanistic studies suggest the reaction is initiated by ligation of the substrate thiolate to the iron centre, and proceeds through an enzyme-bound monocyclic intermediate[3,4] (Fig. 1). Here we report the crystal structure of IPNS complexed to ferrous iron and ACV, determined to 1.3 Å resolution. Based on the structure, we propose a mechanism for penicillin formation that involves ligation of ACV to the iron centre, creating a vacant iron coordination site into which dioxygen can bind. Subsequently, iron-dioxygen and iron-oxo species remove the requisite hydrogens from ACV without the direct assistance of protein residues (Fig. 2). The crystal structure of the complex with the dioxygen analogue, NO and ACV bound to the active-site iron supports this hypothesis.

Spectroscopic studies of IPNS in the resting state have suggested the presence of two or three histidines, an aspartate and possibly two water molecules as metal ligands[5,6]. The crystal structure[7] of *Aspergillus nidulans* IPNS complexed with divalent manganese (substituting for iron) revealed a metal ion octahedrally coordinated by His 214, Asp 216, His 270, Gln 330 and two water molecules (Fig. 3a). Under aerobic conditions, crystals of IPNS bound with both iron and ACV could not be obtained owing to instability and turnover problems. Crystals of IPNS complexed to ferrous iron and ACV were therefore grown under anaerobic conditions[8].

The Fe(II) : ACV : IPNS structure has one protein molecule with ferrous ion and ACV bound at the active site in the asymmetric unit (Fig. 3b). Substrate binding does not distort the 'jelly-roll' core of the enzyme, in which the iron and ACV are enclosed. The side chain of Gln 330, which coordinates the metal in the absence of substrate, is replaced by the ACV thiolate. In the Fe(II) : ACV : IPNS complex, the seven carboxy-terminal residues adopt a conformation that extends the final helix (α-10) relative to the Mn : IPNS structure and encloses the substrate in the active site.

The ACV is anchored within the active site by ligation of its thiolate to the iron centre and through its two carboxylate groups (Fig. 4a). One of the two water molecules ligating the metal ion in the Mn : IPNS complex is displaced, changing the metal coordination geometry from octahedral to square pyramidal (Fig. 2: **4** → **5**). In the substrate complex, three of the five coordination sites are filled with protein ligands: His 214, His 270 and Asp 216 (ref. 9). The remaining two sites are occupied by a water molecule (at position 398) and the ACV thiolate. The valine isopropyl group is held in van der Waals contact with the iron by interactions with Leu 231, Val 272, Pro 283 and Leu 223. The presence of the substrate-derived valine methyl group in the coordination site *trans* to Asp 216 prevents a water molecule from binding. Remarkably, the valine βC–H bond, which is cleaved during the formation of the thiazolidine ring, is directed away from the iron centre. The pentacoordiante and high-spin nature of the Fe(II) : ACV : IPNS complex, and the displacement of one water molecule on ACV binding, were previously inferred from spectroscopic studies[5,6,10].

The aminoadipoyl residue of ACV lies in an extended conformation, as predicted from analogue studies[1,3,11], and its carboxylate makes a salt bridge with Arg 87, replacing that formed between the C-terminal carboxylate (Thr 331) and Arg 87 in the Mn : IPNS structure[12].

The carboxylate of the valine residue of ACV is prevented from coordinating to the iron centre by a hydrogen-bonding network. Before ACV binds, the side chain of Arg 279 points out of the active site towards the exterior of the enzyme (Fig. 3a), but in the Fe(II) : ACV : IPNS structure (Figs 3b and 4a), Arg 279 is directed into the active-site cavity by forming a hydrogen bond to the valine carboxylate of ACV through a bridging water molecule (labelled as

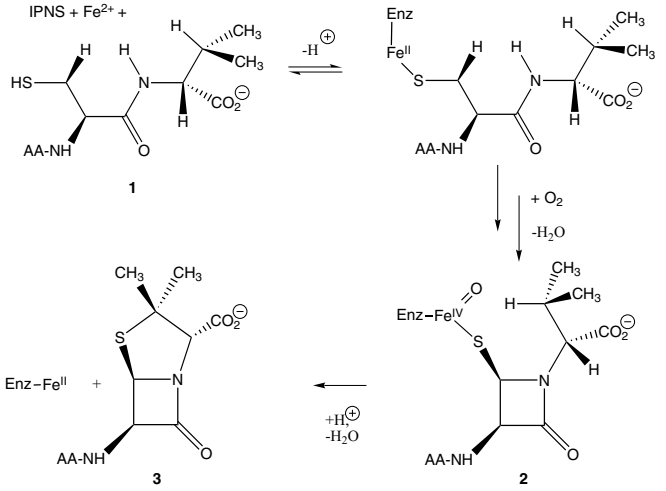

Figure 1 The IPNS reaction pathway through the proposed enzyme (enz)-bound monocyclic intermediate (**2**). AA, *L*-δ-(α-aminoadipoyl).

Table 1 Data collection and statistics

	Fe : (II) : ACV : IPNS		Fe : NO : ACV : IPNS	
X-ray source	BM14, ESRF, Grenoble		ID2, ESRF, Grenoble	
R_{cryst} (%)*	18.2 (8–1.30 Å)		20.66 (25–1.45 Å)	
R_{free} (%)†	19.8		21.2	
Unit Cell	$a = 46.8, b = 71.5, c = 101.0$ Å		$a = 47.26, b = 73.08, c = 101.94$ Å	
Resolution shell	1.35–1.30 Å	25.0–1.3 Å	1.45–1.49 Å	22.0–1.45 Å
Measurements	25,182‡	267,069	10,327	180,036
Average $I/\sigma I$	4.1	25.9	2.3	21.2
Unique reflections	7,714	80,233	3,298	50,924
Completeness (%)	93.2	95.4	85.8	92.0
$I/\sigma I > 3$ data only (%)	52.2	79.2	30.3	69.4
R_{merge} (%)§	31.8	5.5	51.9	8.2

*$R_{cryst} = \Sigma \| |F_{obs}| - |F_{calc}| | / \Sigma |F_{obs}| \times 100$ for the resolution range shown. Figures are for an isotropic, individual B-factor model.
†R_{free} based on 4% of the total reflections.
‡Estimated value.
§$R_{merge} = \Sigma_j \Sigma_h | I_{h,j} - \langle I_h \rangle | / \Sigma_j \Sigma_h \langle I_h \rangle \times 100$, where $I_{h,j}$ is the intensity of an individual measurement and $\langle I_h \rangle$ is the mean intensity of that reflection.

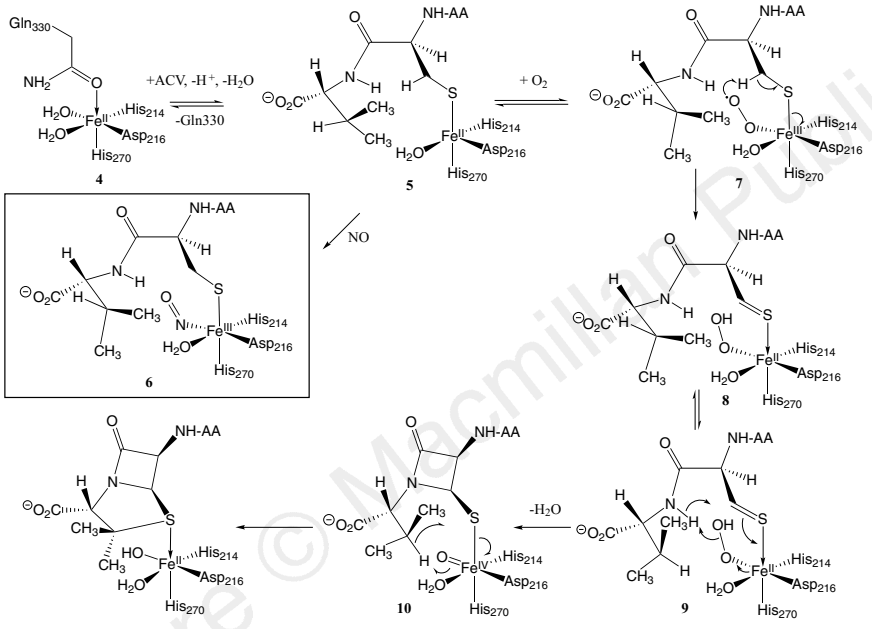

Figure 2 Mechanism for isopenicillin *N* formation and the formation of the Fe : ACV : NO : IPNS complex.

352 in Fig. 4a). The ACV valine carboxylate also forms hydrogen bonds with the side-chain hydroxyls of Ser 281, Tyr 189 and a water molecule (labelled as 567 in Fig. 4a).

Electron paramagnetic resonance (EPR) studies[5] using the dioxygen analogue nitric oxide have indicated that the NO binds to the Fe(II) : ACV : IPNS complex to yield an octahedral complex. When exposed to NO, the crystals of Fe(II) : ACV : IPNS also reacted to form the ternary Fe : NO : ACV : IPNS complex, which has a visible spectrum similar to that observed in solution (λ_{max} for crystals, 507, 715 nm; for solution, 508, 720 nm)[10,13]. The crystal structure of the Fe : NO : ACV : IPNS complex reveals that NO binds to the iron centre *trans* to Asp 216 (Fig. 4b), suggesting that this is the likely oxygen-binding site. To accommodate the NO molecule, a rotation of ~30° occurs around the substrate valine Cα–Cβ bond, increasing the distance between the iron and the ACV-derived valine methyl carbon from 3.90 to 4.81 Å. The NO is bound in a nonlinear orientation (Fe–N–O angle of 120°) and the NO oxygen atom is equidistant (3.3 Å) from both the valine nitrogen and cysteinyl β-carbon, which must each donate a hydrogen atom to dioxygen to close the β-lactam ring.

Ligation of ACV to the iron presumably results in a reduction of the Fe(II)/Fe(III) redox potential, allowing dioxygen to bind, thereby initiating the reaction cycle (Fig. 2). The simplest way to integrate the spectroscopic and structural results is by dioxygen binding in the site *trans* to Asp 216 (**5** → **7**). With a nonlinear, haemoglobin-like binding of dioxygen, the superoxide in **7** is juxtaposed to the *pro*-3-*S* hydrogen of the ACV cysteinyl residue, and could remove this hydrogen atom (**7** → **8**)[14]. Subsequent cleavage of the hydroperoxide with concomitant deprotonation of the amide N–H allows simultaneous β-lactam closure and ferryl formation (**9** → **10**). Rotation of the isopropyl group (**8** → **9**) must occur before or at the same time as β-lactam formation to relieve its steric interactions with the sulphur ligand. This rotation directs the valine β-hydrogen towards the ferryl-oxo species with which it reacts[3,4,15].

The ACV is bound rigidly (ACV average B-factor = 9.3 Å^2; IPNS main-chain average B-factor = 9.9 Å^2) and is held in a conformation in which the cysteinyl carbonyl group eclipses the adjacent Cα–N bond. A torsion angle of −55° is defined by the valine N and by the cysteinyl C-2, C-2 and C-3 of ACV. The tripeptide conformation is therefore approaching that required for β-lactam formation. Examination of the active site fails to reveal any residues capable of providing general acid–base catalysis. Thus the dioxygen has three main roles: as an electron acceptor during β-lactam ring formation; as a source of the ferryl species for the energetically demanding second-ring closure; and to remove specific hydrogen atoms from the substrate directly.

Comparison of the Mn : IPNS and Fe(II) : ACV : IPNS structures shows that, when ACV binds to IPNS, Phe 211 undergoes a 120°

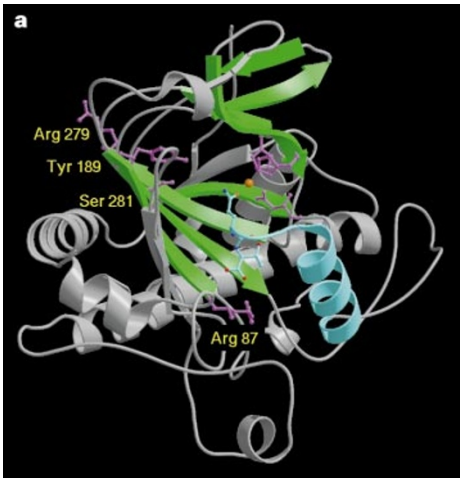

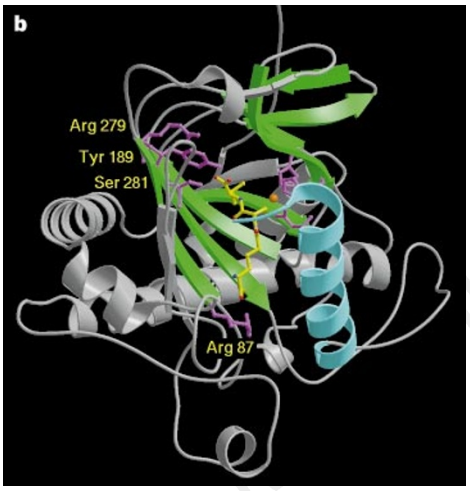

Figure 3 Comparison of the structures of Mn : IPNS (**a**) and Fe(II) : ACV : IPNS (**b**) from the same orientation. The jelly-roll motif is in green, the C-terminal region (residues 313–331) cyan, the active-site metal ion (manganese in **a**, iron in **b**) orange, the key substrate-binding residues (His 214, His 270, Asp 216, Arg 87, Arg 279, Tyr 189 and Ser 281) magenta, and the ACV yellow.

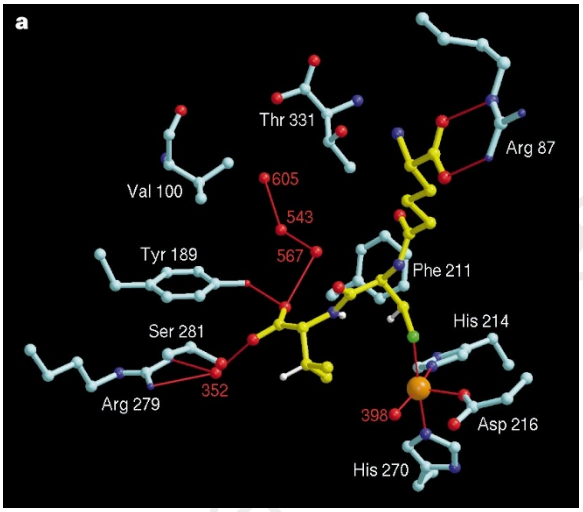

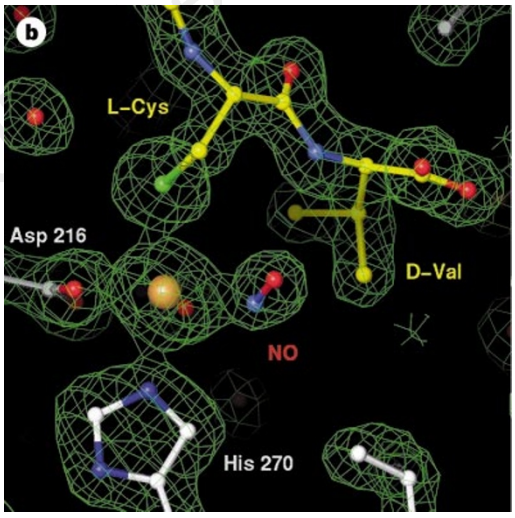

Figure 4 Structure of the active-site region. **a**, The three hydrogen atoms removed to form isopenicillin *N* are shown in white. The iron–sulphur bond length of 2.41 Å observed in this crystal structure is slightly longer than that observed either in solution-phase EXAFS studies[6] of *Cephalosporium acremonium* IPNS 2.32 ± 0.02 Å or in EXAFS studies[8] of the crystalline *A. nidulans* IPNS 2.34 ± 0.03 Å. **b**, Binding of NO to the iron centre. The $2F_o - F_c$ electron density map is contoured at 1.13σ.

rotation about its Cα–Cβ bond, moving the phenyl ring to form part of the active-site cavity (Fig. 3a). In this position, it may help to isolate the proposed hydroperoxide intermediate from potential hydrogen-bonding partners, enhancing the basicity of the hydroperoxide-hydroxide and facilitating deprotonation of the ACV valine N–H. The movement of Phe 211 opens a channel to the protein surface that is bordered by the side chains of Thr 331, Val 100 and Tyr 189 and contains three water molecules (labelled in Fig. 4a as 567, 543 and 605). The water molecule produced when the β-lactam is formed (**9** → **10**) may leave the active site through this channel.

Peroxide and ferryl intermediates have also been proposed in cytochrome P-450 oxygenase and oxidase reactions[16] in which a cysteinyl thiolate may also be the immediate source of electrons for ferryl formation[17]. However, the different geometrical relationships between bound dioxygen and sulphur in the haem and non-haem systems means that they have different reaction pathways. In IPNS, the *cis* sulphur–dioxygen relationship at the iron centre allows the involvement of the ACV-derived cysteinyl moiety in the redox chemistry leading to the β-lactam; in the P-450 enzymes, the *trans* relationship isolates the thiolate from dioxygen so that removal of the 3-cysteinyl hydrogen is not possible. In both cases, however, substrate binding displaces water to create a pentacoordinate iron species before the binding of oxygen. Consequently, although both porphyrin- and non-porphyrin-based catalysts may have evolved to carry out similar oxidative reactions (for example, hydroxylations and desaturations), there may be other reactions (for example, ACV to isopenicillin N) which can only be catalysed by non-haem-based catalysts.

Many (but not all) 2-oxoglutarate-dependent oxygenases and 1-aminocyclopropane-1-carboxylic-acid oxidase (ACCO) show significant sequence similarity to IPNS[7,14,18]. In addition to conservation of the metal-binding ligands corresponding to His 214, Asp 216 and His 270 in IPNS and the predicted tertiary structure (the jelly-roll motif), other residues are conserved across the IPNS subfamily, including Arg 279 and Ser 281, which bind to the ACV valine

carboxylate (Fig. 4a). This carboxylate-binding motif is probably involved in binding the C-5 carboxylate of 2-oxoglutarate, the cosubstrate for all known members of the subfamily except IPNS and ACCO, allowing the C-1 carboxylate of 2-oxoglutarate to coordinate to the iron atom[19].

Sequences reported for Fe(II)-dependent extradiol dioxygenases[20–22] display significant sequence similarity to each other, but not to those of the IPNS subfamily. However, crystallographic studies have shown that the coordination chemistry and proposed mechanism of the extradiol dioxygenases share common features with IPNS. The structure of the Fe(III) form of 2,3-dihydroxybiphenyl dioxygenase with a substrate bound reveals two imidazole (His 209 and His 145) and one carboxylate (Glu 260) metal ligands, with the proposed oxygen-binding site *trans* to the glutamate and the substrate ligated directly to the iron[22]. Thus the IPNS subfamily and the extradiol dioxygenases may have convergently evolved similar solutions to the mechanistic problems posed by using dioxygen as an oxidant. □

Methods

Data collection. All data were collected at 100 K using 0.997-Å radiation and a 30-cm MAR research detector (Table 1).

Structure determination of Fe(II):ACV:IPNS. The Fe(II):ACV:IPNS crystals belong to the space group $P2_12_12_1$. Data were processed with the DENZO and SCALEPACK programs[23], and initial phases were calculated by molecular replacement using the program AMoRe[24]. Electron density maps were interpreted using the program O[25]. In 14 cycles of refinement, using the programs XPLOR[26], PROLSQ[27] and SHELXL93 (ref. 28), 328 residues (4–331) were fitted to the electron density. In the final cycle, the positions of all the atoms in the asymmetric unit, including 322 water molecules, a sulphate ion, the ferrous ion and ACV were refined using SHELXL93 which gave a crystallographic *R*-factor of 13.8% (calculated using anisotropic temperature factors).

Structure determination of Fe:NO:ACV:IPNS. Crystals were prepared under anaerobic conditions by transferring a single coverslip with a drop containing Fe(II):ACV:IPNS crystals to a fresh Linbro crystallization tray, injecting NO gas (1 ml) under the coverslip, and rapidly resealing the well. The crystals reacted by diffusion over 1 h and developed an orange–pink colour. Data from these crystals were processed with MOSFILM[29] and the CCP4 suite of programs[30]. An initial structure was obtained by rigid body refinement of the Fe(II):ACV:IPNS main-chain residues into the new unit cell. In 9 cycles of refinement using REFMAC[30], 327 residues (5–331) were fitted to the electron density. In the final cycle, 116 water molecules, iron, NO and ACV were refined. Electron density for the NO was clearly visible throughout the refinement, and the NO was modelled in after two cycles. For both structures, the iron–ligand bond lengths were unrestrained throughout the refinement, and there were no Ramachandran outliers.

Received 29 January; accepted 15 April 1997.

1. Baldwin, J. E. & Abraham, E. Biosynthesis of penicillins and cephalosporins. *Nat. Prod. Rep.* **5,** 129–145 (1988).
2. Pang, C. P. *et al*. Purification of isopenicillin N synthetase. *Biochem. J.* **222,** 789–795 (1984).
3. Baldwin, J. E. & Schofield, C. J. in *The Chemistry of β-lactams* (ed. Page, M. I.) 1–78 (Blackie, London, 1992).
4. Que, L. & Ho, R. Y. N. Dioxygen activation by enzymes with mononuclear non-haem iron active sites. *Chem. Rev.* **96,** 2607–2624 (1996).
5. Orville, A. M. *et al*. Thiolate ligation of the active site iron(II) of isopenicillin N synthase derives from substrate rather than endogenous cysteine: spectroscopic studies of site-specific Cys → Ser mutated enzymes. *Biochemistry* **31,** 4602–4612 (1992).
6. Randall, C. R. *et al*. X-ray absorption studies of the ferrous active site of isopenicillin N synthase and related model complexes. *Biochemistry* **32,** 6664–6673 (1993).
7. Roach, P. L. *et al*. Crystal structure of isopenicillin *N* synthase is the first from a new structural family of enzymes. *Nature* **375,** 700–704 (1995).
8. Roach, P. L. *et al*. Anaerobic crystallisation of an isopenicillin N synthase.Fe(II).substrate complex demonstrated by X-ray studies. *Eur. J. Biochem.* **242,** 736–740 (1996).
9. Borovok, I., Landman, O., Kreisberg-Zakarin, R., Aharonowitz, Y. & Cohen, G. Ferrous active site of isopenicillin N synthase: genetic and sequence analysis of endogenous ligands. *Biochemistry* **35,** 1981–1987 (1996).
10. Chen, V. J. *et al*. Spectroscopic studies of isopenicillin N synthase. A mononuclear nonhaem Fe^{2+} oxidase with metal coordination sites for small molecules and substrate. *J. Biol. Chem.* **264,** 21677–21681 (1989).
11. Baldwin, J. E. *et al*. Penicillin biosynthesis: active site mapping with aminoadipoylcysteinylvaline variants. *J. Chem. Soc. Chem. Commun.* 1225–1227 (1984).
12. Rowe, C. J. thesis, Oxford Univ. (1995).
13. Hadfield, A. & Hajdu, J. A fast and portable microspectrophotometer for protein crystallography. *J. Appl. Crystallogr.* **26,** 839–842 (1993).
14. Cooper, R. D. G. The enzymes involved in biosynthesis of penicillin and cephalosporin: Their structure and function. *Bioorg. Med. Chem.* **1,** 1–17 (1993).
15. Baldwin, J. E. *et al*. Evidence for an insertion-homolysis mechanism for carbon-sulfur bond formation in penicillin biosynthesis; 2. Incubation and interpretation. *Tetrahedron* **52,** 2537–2556 (1996).
16. Groves, J. T. & Han, Y. Z. in *Cytochrome P-450: Structure, Chemistry and Biochemistry* 2nd edn (ed. Ortiz de Montellano, P. R.) 3–49 (Plenum, New York, 1995).
17. Baldwin, J. E., Morris, G. M. & Richards, W. G. Electron transport in cytochromes P-450 by covalent switching. *Proc. R. Soc. Lond. B* **245,** 43–52 (1991).
18. Prescott, A. G. A dilemma of dioxygenases (or where biochemistry and molecular biology fail to meet). *J. Exp. Bot.* **44,** 849–861 (1993).
19. Hanauske-Abel, H. M. & Guzzler, V. A stereochemical concept for the catalytic mechanism of prolylhydroxylase. *J. Theor. Biol.* **94,** 421–455 (1982).
20. Shu, L. *et al*. X-ray absorption spectroscopic studies of the Fe(II) active site of catechol 2,3-dioxygenase. Implications for the extradiol cleavage mechanism. *Biochemistry* **34,** 6649–6659 (1995).
21. Han, S., Eltis, L. D., Timmis, K. N., Muchmore, S. W. & Bolin, J. T. Crystal structure of the biphenyl-cleaving extradiol dioxygenase from a PCB-degrading pseudomonad. *Science* **270,** 976–980 (1995).
22. Senda, T. *et al*. Three-dimensional structures of free form and two substrate complexes of an extradiol ring-cleavage type dioxygenase, the BphC enzyme from *Pseudomonas* sp. strain KKS102. *J. Mol. Biol.* **255,** 735–752 (1996).
23. Otwinowski, Z. in *Data Collection and Processing* (eds Sawyer, L., Isaacs, N. W. & Bailey, S.) 55–62 (Daresbury Laboratory, Warrington, UK, 1993).
24. Navaza, J. AMoRe: an automated package for molecular replacement. *Acta Crystallogr. A* **50,** 157–163 (1994).
25. Jones, T. A., Zou, J. Y., Cowan, S. W. & Kjelgaard, M. Improved methods for building protein models in electron density maps and the location of errors in these models. *Acta Crystallogr. A* **47,** 110–119 (1991).
26. Brünger, A. T., Kuriyan, J. & Karplus, M. Crystallographic R factor refinement by molecular dynamics. *Science* **235,** 458–460 (1987).
27. Konnert, J. H. & Hendrickson, W. A. A restrained-parameter thermal-factor refinement procedure. *Acta Crystallogr. A* **36,** 344–350 (1980).
28. Sheldrick, G. M. *SHELXL93, Program for Crystal Structure Refinement* (Univ. Gottingen, Germany, 1993).
29. Leslie, A. G. W. *Mosflm* (MRC Laboratory of Molecular Biology, Cambridge, 1996).
30. CCP4 The CCP4 suite: programs for protein crystallography. *Acta Crystallogr. D* **50,** 760–763 (1994).

Acknowledgements. We thank K. Harlos, E. Garman, R. Bryan, I. Andersson, R. M. Adlington, R. C. Wilmouth, V. Fülöp, J. P. N. Pitt, A. Howe, S. Lee, J. W. Keeping, B. Rasmussen and A. Thompson for help and discussions. Financial support was provided by the MRC, BBSRC, EPSRC and Zeneca through a DTI link scheme.

Correspondence and requests for materials should be addressed to J.E.B. or J.H. The crystallographic coordinates have been deposited in the Brookhaven Protein Data Bank (accession nos 1IPS, 2IPS and 3IPS) and will be released one year after publication.

erratum

Photonic crystals: putting a new twist on light

J. D. Joannopoulos, Pierre R. Villeneuve & Shanhui Fan

Nature **386,** 143–149 (1997)

Figure 6 in this Review was shown in the wrong orientation. The figure as printed should be rotated 90° anticlockwise. □